ARTICLE

BIOTECHNOLOGY and BIOENGINEERING

Metabolic Flux Analysis for Recombinant Protein Production by *Pichia pastoris* Using Dual Carbon Sources: Effects of Methanol Feeding Rate

Eda Çelik,[1] Pınar Çalık,[1] Stephen G. Oliver[2]

[1]Department of Chemical Engineering, Industrial Biotechnology and Metabolic Engineering Laboratory, Middle East Technical University, 06531 Ankara; telephone: 90-312-210-43-85; fax: 90-312-210-26-00, Turkey; e-mail: pcalik@metu.edu.tr

[2]Department of Biochemistry, University of Cambridge, Cambridge, UK

Received 8 June 2009; revision received 18 August 2009; accepted 11 September 2009

Published online 23 September 2009 in Wiley InterScience (www.interscience.wiley.com). DOI 10.1002/bit.22543

ABSTRACT: The intracellular metabolic fluxes through the central carbon pathways in the bioprocess for recombinant human erythropoietin (rHuEPO) production by *Pichia pastoris* (Mut^+) were calculated to investigate the metabolic effects of dual carbon sources (methanol/sorbitol) and the methanol feed rate, and to obtain a deeper understanding of the regulatory circuitry of *P. pastoris*, using the established stoichiometry-based model containing 102 metabolites and 141 reaction fluxes. Four fed-batch operations with (MS-) and without (M-) sorbitol were performed at three different constant specific growth rates (h^{-1}), and denoted as M-0.03, MS-0.02, MS-0.03, and MS-0.04. Considering the methanol consumption pathway, the M-0.03 and MS-0.02 conditions produced similar effects and had >85% of formaldehyde flux towards the assimilatory pathway. In contrast, the use of the dual carbon source condition generated a shift in metabolism towards the dissimilatory pathway that corresponded to the shift in dilution rate from MS-0.03 to MS-0.04, indicating that the methanol feed exceeded the metabolic requirements at the higher μ_0. Comparing M-0.03 and MS-0.03 conditions, which had the same methanol feeding rates, sorbitol addition increased the rHuEPO synthetic flux 4.4-fold. The glycolysis, gluconeogenesis, and PPP pathways worked uninterruptedly only at MS-0.02 condition. PPP and TCA cycles worked with the highest disturbances at MS-0.04 condition, which shows the stress of increased feeding rates of methanol on cell metabolism.

Biotechnol. Bioeng. 2010;105: 317–329.

KEYWORDS: *Pichia pastoris*; flux; sorbitol; methanol; metabolism; fed-batch

Introduction

The methylotrophic yeast *Pichia pastoris* has become a popular host for industrial protein production due to its ability to produce foreign proteins at high levels. An overview of the literature on recombinant-protein (r-protein) production by *P. pastoris* reveals the importance of the proper choice of carbon source(s) and their feeding strategy. This is mainly due to the fact that methanol is the inducer of the *AOX1* promoter, and hence r-protein production, but is toxic at high levels. A typical three-stage methanol fed-batch operation has been commonly used. On the other hand, a fed-batch strategy using mixed substrates of glycerol and methanol for *P. pastoris* was proposed to increase productivity, cell density, and reduce the induction time (Brierley et al., 1990). However, the optimal level of protein expression is not achievable with mixtures of glycerol and methanol due to a partial repression of the *AOX1* promoter by glycerol, which may result in lower specific productivities of r-protein (Hellwig et al., 2001; Sreekrishna et al., 1997; Xie et al., 2005). An alternate strategy exploits sorbitol, which is a non-repressing carbon source for the *AOX1* promoter (Inan and Meagher, 2001; Sreekrishna et al., 1997), thus sorbitol accumulation during the induction phase does not affect the expression level of r-protein. These advantages, although widely utilized for Mut^S (methanol utilization slow) strains, have not been appreciated for Mut^+ (methanol utilization positive) strains, and only utilized in a limited number of studies (Inan and Meagher, 2001; Jungo et al., 2007; Ramon et al., 2007; Sreekrishna et al., 1997).

Recently, we (Çelik et al., 2009) proposed a new production strategy using *P. pastoris* Mut^+ strains, where batch-wise addition of sorbitol as a co-substrate, at the induction phase of a methanol fed-batch fermentation, was found to be beneficial. However, to gain deeper insights and to fine-tune bioreactor performance further, the influence of the carbon sources and the feeding strategy on the

Correspondence to: Pınar Çalık

Contract grant sponsor: Scientific and Technological Research Council of Turkey (TÜBİTAK)
Contract grant number: 107M285
Contract grant sponsor: METU Research Fund
Contract grant sponsor: UK Biotechnology & Biological Sciences Research Council

intracellular reaction network of r-*P. pastoris* needs to be clarified. An analysis of the distribution of the intracellular biochemical reaction-network fluxes during the growth, product and by-product formation should provide new information for understanding the physiological characteristics of the organism and reveal important features of the regulation of the intracellular bioreaction network (Çalık and Özdamar, 1999; Çalık et al., 1999).

The literature on metabolic flux analysis (MFA) on *P. pastoris* is limited to just two studies (Sola et al., 2004, 2007). Sola et al. (2004) determined the amino acid biosynthesis and central carbon metabolism fluxes of *P. pastoris* by stable isotope labeling experiments in glycerol-containing medium, and compared them with those of *Saccharomyces cerevisiae*. They concluded that amino acids synthesis and regulation of central carbon metabolism in *P. pastoris* were similar to *S. cerevisiae*. In their latter study, the methanol utilization pathway was also included in the analysis and Sola et al. (2007) concluded that metabolic flux balancing analysis will lead to important insights into the central metabolism and its regulation in *P. pastoris*. However, the response of metabolism to r-protein production was missing in these studies. On the other hand, although there is no work on fed-batch metabolic flux distribution by *P. pastoris*, such studies have been undertaken with *Penicillium chrysogenum* (Jorgensen et al., 1995), *S. cerevisiae* (Chen et al., 1994; Toivari et al., 2001), and *Escherichia coli* (Antoniewicz et al., 2007; Nöh et al., 2007; Tsai et al., 1996; Van De Walle and Shiloach, 1998; Van Wegen et al., 2001).

In this context, the aim of the present work is to investigate the regulatory effect of methanol feeding in the presence and absence of sorbitol on metabolic flux distributions of *P. pastoris* producing recombinant human erythropoietin (rHuEPO) in a fed-batch fermentation process, using a mass flux balance-based analysis to obtain deeper insights into the regulation of the intracellular bioreaction network and reveal potential metabolic bottlenecks for r-protein production using *P. pastoris*.

Materials and Methods

Strain and Growth Conditions

P. pastoris-E17 Mut$^+$ strain carrying EPO cDNA under the control of *AOX1* promoter (Çelık et al., 2007) was maintained and cultivated as described previously (Çelik et al., 2009). Fed-batch r-protein production was carried out in 3.0 L pilot-scale bioreactor (Braun CT2-2) as given in detail elsewhere (Çelik et al., 2009). The defined production medium initially contained per liter: 40 g glycerol; 26.7 mL H_3PO_4 (85%); 14.9 g $MgSO_4{\cdot}7H_2O$; 0.93 g $CaSO_4$; 18.2 g K_2SO_4; 4.13 g KOH; 4.35 mL of PTM1 salt solution; and 0.1 mL antifoam (Y-30 emulsion, Sigma (St Louis, MO)). Four fed-batch runs were performed, having identical precultivation phases until the methanol-induced production phase. For a constant specific growth rate, μ_0, of $0.03\,h^{-1}$, production was carried out without sorbitol, and this run was denoted as the M-0.03 condition. In the other three fed-batch operations with sorbitol, at the beginning of the production phase, sorbitol was added to the medium in the batch phase, prior to feeding, such that $C_{S0} = 50$ g/L. Methanol was then fed to the system at a predetermined rate for $\mu_0 = 0.02\,h^{-1}$, $\mu_0 = 0.03\,h^{-1}$, and $\mu_0 = 0.04\,h^{-1}$, and these conditions were denoted as MS-0.02, MS-0.03, and MS-0.04, respectively.

Analyses

The methods of Çelik et al. (2009) were used to measure the concentration of biomass, glycerol, methanol, sorbitol, and rHuEPO; total protein concentration was determined by the Bradford assay (Bradford, 1976). Excreted amino acid concentrations were measured with an amino acid analysis system (Waters HPLC, Milford, MA), using the modified Pico Tag method (Çalık et al., 1998). Excreted organic acid concentrations were measured with an HPLC (Waters-2695) (İleri and Çalık, 2006; Çelık et al., 2008). Yeast viability was assessed by methylene blue staining (Bonora and Mares, 1982). All analyses were performed at least in duplicate.

Mass Flux Balance-Based Analysis

The intracellular biochemical reaction network of *P. pastoris* was constructed based on the metabolism of the model yeast *S. cerevisiae* (Förster et al., 2003; Kresnowati et al., 2008; Maaheimo et al., 2001), the central metabolism of which has also been shown to be suitable for *Pichia stipitis* (Fiaux et al., 2003) and *P. pastoris* (Sola et al., 2004, 2007), as well as the recently annotated *P. pastoris* genome (De Schutter et al., 2009). The map of the metabolic reaction network and the stoichiometric reactions of the network, consisting of $m = 102$ metabolites and $n = 141$ reactions, are given in Figure 1 and in the Appendix. The overall pathway was simplified by lumping some reactions into single ones without losing representation accuracy.

The following major assumptions are used in the model: (i) all the recombinant cells were assumed to perform identically throughout the bioprocess; (ii) the genetic structure, genetic control mechanisms and the regulation of the intracellular bioreaction network of the genetically engineered yeast were assumed to be directed towards the desired protein in response to the designed environment; and the transcription and translation steps for r-protein synthesis and secretion of the r-protein were non-limiting; (iii) the amino acid and organic acid excretion and transportation processes were assumed to proceed via passive transport; (iv) CO_2, NH_3, in the form of NH_4^+, and phosphate transport from the cell to the broth and from the broth to the cell were also assumed to be by passive transport (Çalık and Özdamar, 2002b); (v) $P/O = 2$ for *S. cerevisiae* (Nielsen et al., 2003) was assumed to be valid for *P. pastoris*;

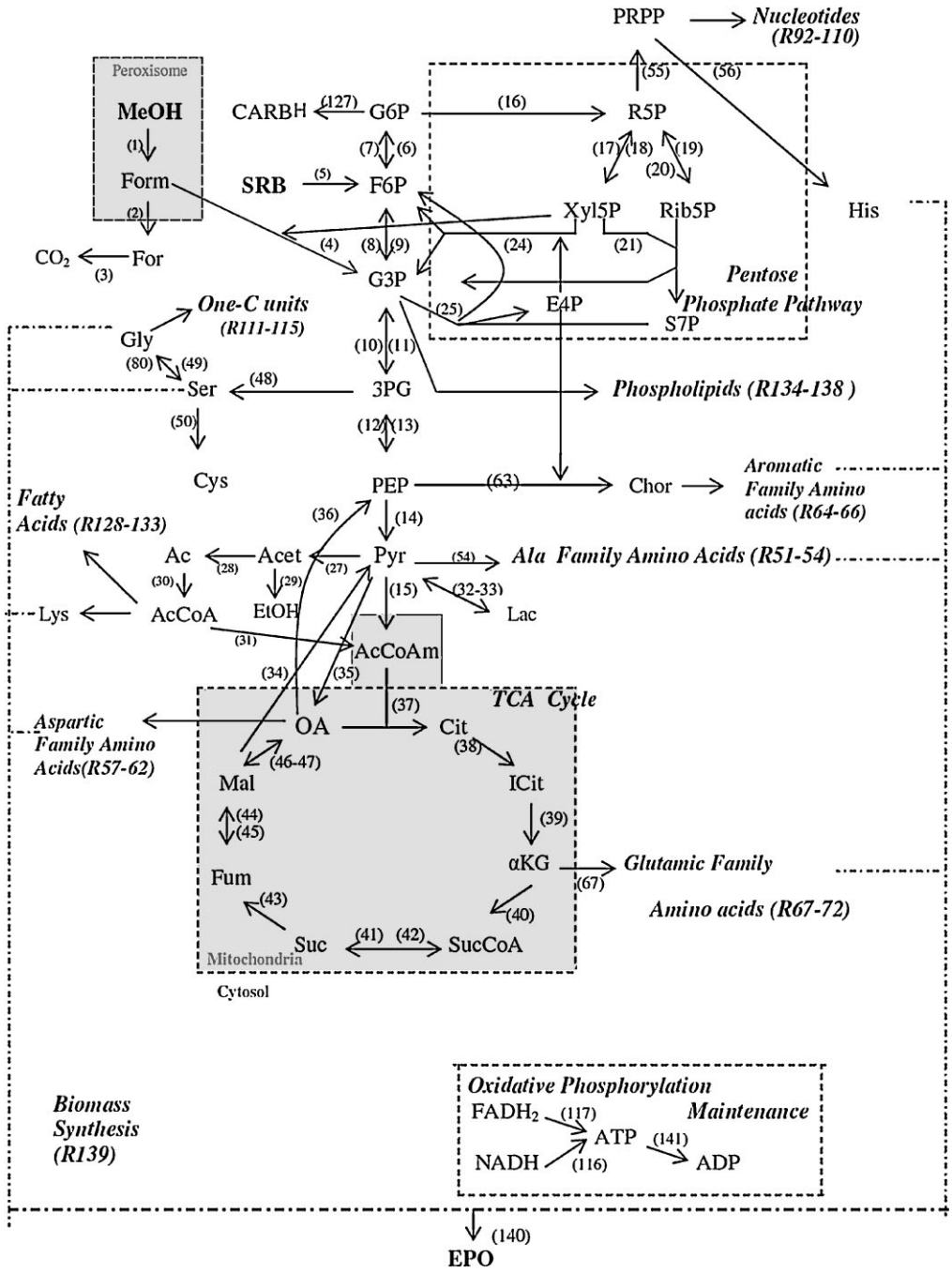

Figure 1. The metabolic pathway map of *P. pastoris* producing rHuEPO.

(vi) compartmentation into cytosol and mitochondria was considered for metabolites (acetyl-CoA, NADPH, and NADH) that cannot cross the mitochondrial membrane in both directions (Förster et al., 2002); (vii) the biomass synthesis reaction (R139) was written by considering the macromolecular composition of *S. cerevisiae* (Förster et al., 2003); (viii) the glyoxylate cycle was considered inactive (Gonzalez et al., 2003; Sola et al., 2007); (ix) the recently annotated (De Schutter et al., 2009) lactate dehydrogenases (protein ID: XP_002491260.1 and XP_002492901.1) were considered to be responsible for the lactate metabolism given by R32 and R33, respectively. Although the former protein is encoded by a putative ldhA gene of *P. pastoris* (not annotated in *S. cerevisiae*), considering the fact that ethanol does not accumulate in *P. pastoris* medium (Cereghino and Cregg, 2000), a direct reduction of the intracellular pyruvate

to lactate could be the alternative pathway for the NAD^+ regeneration. Thus, lactate was included in the model, since its accumulation was previously observed in *P. pastoris* extracellular medium (Çelik et al., 2009; Xie et al., 2005).

Moreover, it should be noted that, in writing the rHuEPO synthesis reaction (R140), the amino acid components and the ATP requirements for peptide bond formation between these amino acids were calculated by considering the intracellular composition of the protein, not the mature form. Knowing that 4 ATP-equivalents are required per peptide bond formation (Mathews and van Holde, 1996), a total of 266 amino acids would require 1,064 ATP (R140).

The optimization program GAMS 2.25 (General Algebraic Modeling System, GAMS Development Corp., Washington, DC) was used to solve the mass-flux balance equation:

$$A * r(t) = c(t) \tag{1}$$

where **A** is the stoichiometric coefficients matrix of the metabolic network, $\mathbf{r}(t)$ the vector of fluxes, and $\mathbf{c}(t)$ the extracellular metabolite accumulation vector. Due to the very high turnover of the pools of most metabolites, their concentrations rapidly adjust to new levels making it reasonable to use pseudo-steady state (PSS) approximation for the intracellular metabolites; thus considering only the extracellular accumulation of metabolites (Çalık and Özdamar, 2002a). As rHuEPO is an extracellular recombinant gene product that is secreted to the medium when the polypeptide chain synthesis is completed, the model was solved by minimizing the rHuEPO accumulation-rate in the cell. The model variables (reaction-fluxes) were expressed in mmol/g DW/h; and the flux towards biomass was represented by the specific growth rate (μ) in h^{-1}.

Results and Discussion

Fed-Batch Cultivations and Metabolic Flux Data

In our previous article (Çelik et al., 2009), we systematically investigated the metabolic response of *P. pastoris* Mut^+ cells to methanol feeding in the presence of sorbitol via four fed-batch runs at different dilution rates and monitored the production of cells, r-protein, alcohol oxidase and protease, as well as by-product formation and carbon source consumption. The variations in cell, rHuEPO, protease, sorbitol concentrations and specific alcohol oxidase activity with the cultivation time are summarized in Figure 2 for MS-0.03 (dual substrate, $\mu_0 = 0.03\ h^{-1}$) condition, to demonstrate the three representative periods selected for MFA. To analyze each period, a screenshot of the metabolism is taken, that is extracellular concentration data (Çelik et al., 2009) from representative points of each period are used in the MFA. Period I ($0 < t < 6$ h) includes the lag phase, where the AOX enzyme reaches its maximum and rHuEPO synthesis just starts to increase; Period II ($6 < t < 12$ h) is the exponential phase where the rHuEPO and cell synthesis rates were at their highest; and Period III ($t > 12$) is the diminution phase for rHuEPO and cell synthesis, the start of protease production, as well as the end of the sorbitol consumption period. The data for cultivation times of $t_1 = 4.5$ h, $t_2 = 9$ h, and $t_3 = 15$ h

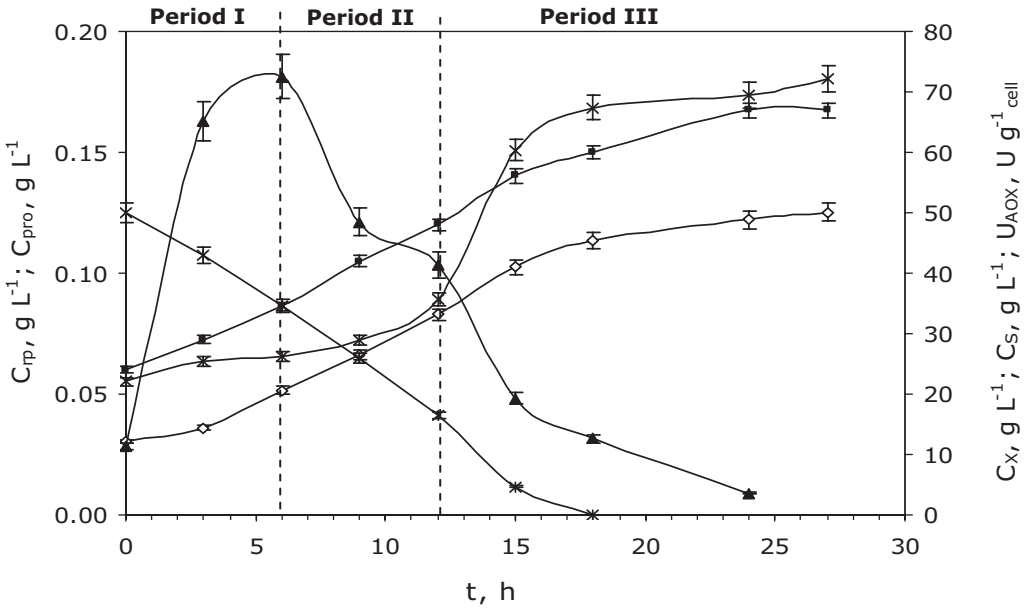

Figure 2. Variations in biomass and metabolite concentrations with the cultivation time for MS-0.03 condition, and the three periods of the bioprocess. RHuEPO concentration, C_{rp} (◇); protease concentration, C_{pro} (x); cell concentration, C_X (■); sorbitol concentration, C_S (*); specific AOX activity, U_{AOX} (▲).

were used to obtain the intracellular metabolic flux distributions in Periods I, II, and III, respectively. The yeast viability was almost 100% in glycerol medium, always above 95% in sorbitol containing medium, and above 90% in medium containing solely methanol, indicating that the mixing of intracellular components with extracellular components due to cell lysis can be neglected.

Metabolic Flux Analysis for the M-0.03 Condition

The intracellular fluxes were normalized with respect to methanol uptake flux (R1) and denoted as C-mol percentage (C-mol/C-mol MeOH), to analyze the metabolic flux distribution around the glycolysis pathway (Fig. 3) easily and without the contribution of different starting conditions. In all the periods of M-0.03 condition, methanol was converted to formaldehyde (via R1, with 3.345, 3.787, 3.998 mmol/g DW/h for Periods I, II, III, respectively) and a higher fraction of formaldehyde (>85% of the total formaldehyde synthesis flux) entered the assimilatory pathway (via R4) to be converted to other metabolites, rather than being discarded by the dissimilatory pathway (R2–R3) (Fig. 3). Since the entrance of the sole carbon source (methanol) to the metabolism is from G3P, above this point the gluconeogenesis pathway was active, and below this point the glycolysis pathway was active, as expected. In Period II, there was a breakdown of the glycolysis pathway at R14 (=0 mmol/g DW/h), and pyruvate (Pyr) was replenished by the anaplerotic reaction R34, with a flux of 0.232 mmol/g DW/h. The pentose phosphate pathway (PPP) was active in all the periods; however, the route for the formation of the key intermediate, R5P, used for the synthesis of the nucleotides and biomass components, changed throughout the cultivation period. Moreover, its synthesis rate decreased with cultivation time 2.3-fold in Period II, and 23.8-fold in Period III as compared to Period I (Fig. 3).

Most of the branches from the tricarboxylic acid (TCA) cycle (R27, R28, R29, R30, R33) were inactive. Ethanol and acetate synthesis fluxes (R28, 29) both were zero, which was also consistent with the findings of other studies (Sola et al., 2007). While, in the early periods of the bioprocess, Pyr and phosphoenolpyruvate (PEP) were replenished through the anaplerotic reactions R34 and R36, oxaloacetate (OA) was required more at later time and was supplied by the anaplerotic reaction R35. Moreover, the TCA cycle was not complete in all the periods, probably due to oxygen supply not meeting the oxygen demand (Çelik et al., 2009).

In Periods II and III the flux for Glu synthesis was the highest (1.816 and 0.243 mmol/g DW/h, respectively); and in Period I, the highest synthesis flux was obtained with proline (Pro), which was later converted again to Glu by R85 (=3.273 mmol/g DW/h). In fact, the central importance of Glu lies in the fact that it is used for the synthesis of many other amino acids, that is, Ser, Pro, Arg, Asp, alanine (Ala), valine (Val), leucine (Leu), isoleucine (Ile), phenylalanine (Phe), tyrosine (Tyr), glutamine (Gln), and lysine (Lys).

Considering all the conditions investigated, only in the M-0.03 condition was ATP not generated via oxidative phosphorylation of $FADH_2$ (Table II). Under this condition, ATP was mostly synthesized via oxidative phosphorylation of NADH and its rate of synthesis decreased with the cultivation time. Almost half of the ATP produced was consumed for maintenance in Period I. Biomass (R139) and rHuEPO (R140) fluxes increased throughout the periods, due to the long lag phase observed in the M-0.03 condition, and reached R139 = 0.028 mmol/g DW/h and R140 = 0.0059 μmol/g DW/h in Period III.

Metabolic Flux Analysis for the MS-0.02 Condition

Considering the metabolism of methanol, almost all of the formaldehyde (>99%) entered the assimilatory pathway to be converted to other metabolites in all the periods, rather than being discarded by the dissimilatory pathway (Fig. 3). This shows that, only in this condition, did the methanol feed not exceed the cells' requirements. The glycolysis, gluconeogenesis, and PPP pathways worked uninterruptedly in all the periods. However, the synthesis of the key intermediate, R5P, was severely diminished throughout the cultivation and attained a value of 2.9% C-mol R5P/C-mol MeOH in Period III (Fig. 3).

From the anaplerotic reactions, the Pyr and OA replenishment reactions (R34, R35) were active at all times. The TCA cycle was complete only in the first period. Tyr was not synthesized throughout the bioprocess (Table I), but was supplied by the catabolism reaction R84. Thus, adding tyrosine to the medium in MS-0.02 condition could be helpful in improving the protein synthesis pathway. Other than Tyr, all other amino acids were synthesized in Periods I and II, while Trp and cysteine (Cys) were also not synthesized in Period III. There was a general trend of decrease in the amino acid synthesis fluxes, and Glu, of central importance for precursor supply, again had the highest synthesis flux (0.943 mmol/g DW/h in Period I) and with the same supply route as in M-0.03 condition.

The nucleotide (R92–110), carbohydrate (R127) and lipid synthesis (R128–138) pathway fluxes in Period I were the highest of all conditions. ATP was supplied by increasing the contribution of substrate-level phosphorylation reactions (R10, R14, and R41) and decreasing the contribution of oxidative phosphorylation reactions (R116 and R117) throughout the cultivation (Table II). The maintenance energy requirement always had the greatest value in Period I. Moreover, the highest rHuEPO synthesis flux (R140 = 0.0068 μmol/g DW/h) was obtained for Period II compared to the other conditions, which was twice the flux for the M-0.03 condition, but only slightly higher than the other conditions. On the other hand, the lowest flux to r-protein of all the conditions was observed in the last period (R140 = 0.0020 μmol/g DW/h).

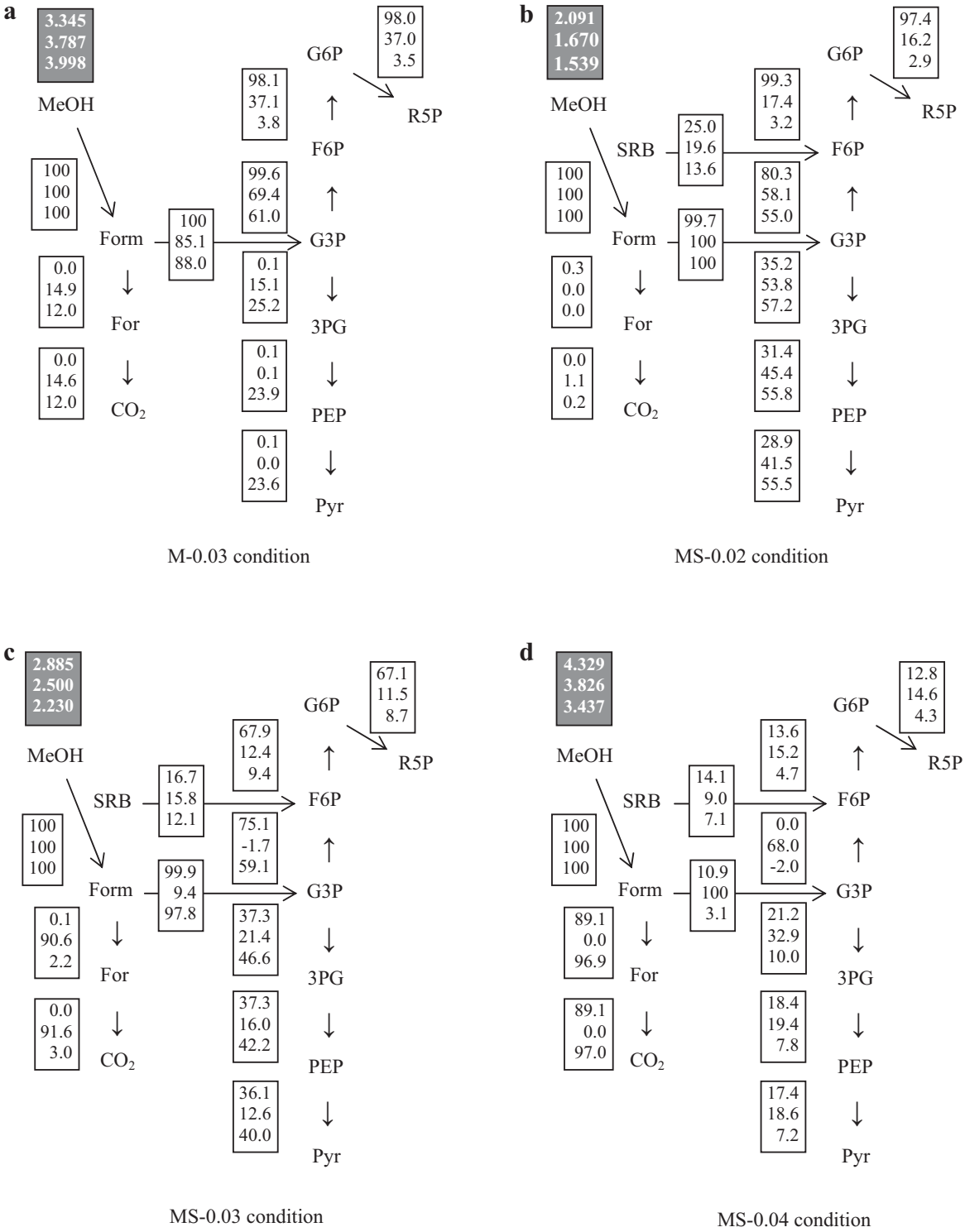

Figure 3. Metabolic flux distributions around the glycolysis pathway. The gray-colored boxes show the actual methanol uptake fluxes (R1) in mmol/g DW/h. The upper, middle, and lower values in the clear boxes correspond to the metabolic fluxes normalized with respect to methanol uptake flux (%, C-mol/C-mol MeOH) obtained in Periods I, II and III, respectively.

Table I. Variation in intracellular amino acid fluxes with feeding condition and cultivation period.

	M-0.03 condition fluxes (mmol/g DW/h)			MS-0.02 condition fluxes (mmol/g DW/h)			MS-0.03 condition fluxes (mmol/g DW/h)			MS-0.04 condition fluxes (mmol/g DW/h)		
Ammo acid	Period I	Period II	Period III	Period I	Period II	Period III	Period I	Period II	Period III	Period I	Period II	Period III
Ala	0.0007	0.0040	0.0130	0.0440	0.0010	0.0050	0.0270	0.0000	0.0000	0.0380	0.0260	0.0180
Arg	0.0000	0.2260	0.0040	0.0150	0.0080	0.0020	0.2540	0.0080	0.0060	0.0380	0.0090	0.0060
Asn	0.0000	0.0020	0.0030	0.0100	0.0050	0.0010	0.0050	0.0050	0.0040	0.0070	0.0060	0.0040
Asp	0.0000	0.7520	0.1030	0.5530	0.1850	0.0350	1.3330	0.1750	0.1270	0.3870	0.4960	0.1310
Cys	0.0000	0.0001	0.0002	0.0007	0.0010	0.0000	0.0040	0.0000	0.0000	0.0006	0.2360	0.0000
Gln	0.0060	0.2700	0.0890	0.2690	0.1820	0.0300	0.4180	0.1760	0.1270	0.2560	0.4680	0.1090
Glu	0.0006	1.8160	0.2430	0.9430	0.4620	0.0940	2.0170	0.4600	0.3250	0.8260	1.2020	0.3350
Gly	0.0050	0.0000	0.0490	0.0550	0.1080	0.0200	0.0000	0.0980	0.0720	0.1010	0.2670	0.0680
His	0.0003	0.0010	0.0180	0.0060	0.0030	0.0007	0.0050	0.0030	0.0020	0.0050	0.0930	0.0030
Ile	0.0050	0.0020	0.0060	0.0220	0.0090	0.0020	0.0110	0.0100	0.0070	0.0160	0.0110	0.0080
Leu	0.0010	0.0020	0.0600	0.0290	0.1080	0.0180	0.0170	0.0950	0.0690	0.1880	0.4020	0.0120
Lys	0.0010	0.0030	0.0070	0.0270	0.0180	0.0030	0.0180	0.0150	0.0100	0.0230	0.0470	0.0110
Met	0.0003	0.0005	0.0020	0.0070	0.0030	0.0008	0.0040	0.0040	0.0020	0.0060	0.0040	0.0030
Phe	0.0005	0.0010	0.0040	0.0230	0.0110	0.0030	0.0080	0.0070	0.0050	0.0110	0.0080	0.0050
Pro	3.2730	0.0020	0.0040	1.2820	0.0080	0.0020	0.0100	0.0090	0.0060	0.0130	0.0090	0.0060
Ser	0.0000	0.5680	0.0520	0.0770	0.1400	0.0220	0.0000	0.1340	0.0970	0.1210	0.5170	0.0770
Thr	0.0030	0.4940	0.0100	0.2780	0.0180	0.0040	0.9100	0.0200	0.0140	0.1260	0.0220	0.0190
Trp	0.0009	0.0005	0.0000	0.0040	0.0220	0.0000	0.0030	0.0260	0.0170	0.0030	0.0010	0.0007
Tyr	0.0020	0.0008	0.0030	0.0000	0.0000	0.0000	0.0060	0.0090	0.0040	0.0080	0.0060	0.0040
Val	0.0010	0.0020	0.0080	0.0260	0.0130	0.0030	0.0150	0.0140	0.0140	0.0220	0.0320	0.0100
Total	3.3003	4.1469	0.6782	3.6707	1.3050	0.2455	5.0650	1.2680	0.9080	2.1956	3.8620	0.8297

Metabolic Flux Analysis for the MS-0.03 Condition

In methanol metabolism, almost all of the formaldehyde entered the assimilatory pathway and was converted to other metabolites in Periods I and III, whereas most (91%) was discarded by the dissimilatory pathway in Period II (Fig. 3). This fluctuation shows that the methanol feed was in excess of the metabolic requirements in general, but especially in Period II. The glycolysis, gluconeogenesis, and PPP pathways worked uninterruptedly in Periods I and III, and was similar to MS-0.02 condition. However, in the exponential phase (Period II), the glycolysis reaction from F6P to G3P was active, rather than the reverse (shown by a negative flux in Fig. 3), since sorbitol enters metabolism. This shows that the requirement for sorbitol increases in the exponential growth phase. Moreover, the PPP was mostly inactive in this period, and R5P had a low synthesis flux.

Most of the branches from the TCA cycle (R27, R28, R29, R30, R33) were inactive, and from the anaplerotic reactions, Pyr and OA replenishment reactions (R34, R35) were active at all times, similar to other sorbitol-containing conditions. The TCA cycle was complete only in Period I. Compared to M-0.03 condition, where TCA was not completed in all the periods, sorbitol addition proves to improve the oxygen insufficiency caused by methanol consumption and consequently repairs the TCA cycle. In Periods I and III, the highest total intracellular amino acid flux was obtained, being 5.065 and 0.908 mmol/g DW/h, respectively. In Period I, Ser and Gly; in Periods II and III, Cys and Ala were supplied through catabolism reactions, given that the fluxes for synthesis reactions of these amino acids were zero (Table I). Glutamatic acid, the amino acid of central importance, again had the highest intracellular flux. The nucleotide synthesis pathway fluxes were the highest of all conditions in Period III.

The highest ATP synthesis rate, comparing all three conditions, was achieved in Period II, where it was supplied mostly by oxidative phosphorylation, R116 (Table II). Moreover, in Period II, the highest maintenance energy requirements were also observed (R141 = 9.59 mmol/g DW/h). On the other hand, in the other periods, substrate-level phosphorylation had a higher impact and ATP was not wasted for maintenance energy requirements.

Metabolic Flux Analysis for the MS-0.04 Condition

Following methanol metabolism, only in Period II was all of the formaldehyde produced channeled into the assimilatory pathway for conversion to other metabolites, while most (>89%) of it was discarded by the dissimilatory pathway in Periods I and III (Fig. 3). This fluctuation shows that the methanol feed rate was too high at the start of the process, where the cells are still in the late adaptation phase. Thus, when *P. pastoris* induction medium is supplemented with sorbitol as the co-substrate, the predetermined feed rate of methanol (Çelik et al., 2009) does not need to be higher than that required for $\mu_0 = 0.04\,h^{-1}$. On the other hand, both glycolysis and gluconeogenesis worked efficiently in Periods II and III (Fig. 3). PPP was mostly inactive in Periods I and III, and the R5P synthesis fluxes were generally low compared to other conditions.

The TCA cycle was not complete in any of the periods, thus oxygen insufficiency was the highest for this condition,

Table II. Variation in ATP generated throughout the bioprocess with feeding condition.

	Amount of ATP produced (mmol/g DW/h)			Percent of ATP produced (%)		
R#	Period I	Period II	Period III	Period I	Period II	Period III
M-0.03 condition						
10	0.005	0.573	1.008	0.1	14.8	29.1
14	0.002		0.942	0.0	0.0	27.2
41	0.004	0.002	0.000	0.1	0.1	0.0
106	0.000	0.000	0.002	0.0	0.0	0.1
108	0.000	0.000	0.001	0.0	0.0	0.0
116	3.310	3.283	1.459	50.1	85.1	42.1
117	3.284		0.052	49.7	0.0	1.5
Total	6.61	3.86	3.46	100	100	100
MS-0.02 condition						
10	0.735	0.899	0.881	12.3	28.9	40.7
14	0.605	0.693	0.854	10.2	22.3	39.5
41	0.003	0.001	0.002	0.1	0.0	0.1
106	0.005	0.003	0.001	0.1	0.1	0.0
108	0.003	0.001	0.000	0.1	0.0	0.0
116	3.336	1.402	0.412	56.0	45.0	19.0
117	1.270	0.115	0.014	21.3	3.7	0.6
Total	5.96	3.11	2.16	100	100	100
MS-0.03 condition						
10	1.075	0.535	1.039	16.0	7.7	33.1
14	1.042	0.316	0.891	15.5	4.6	28.4
41	0.244		0.005	3.6	0.0	0.2
106	0.003	0.003	0.002	0.0	0.0	0.1
108	0.002	0.002	0.001	0.0	0.0	0.0
116	4.123	5.963	1.119	61.2	86.1	35.6
117	0.244	0.103	0.085	3.6	1.5	2.7
Total	6.73	6.92	3.14	100	100	100
MS-0.04 condition						
10	0.918	1.258	0.343	7.7	21.8	4.2
14	0.753	0.712	0.247	6.3	12.3	3.1
41		0.017		0.0	0.3	0.0
106	0.005	0.003	0.002	0.0	0.1	0.0
108	0.003	0.002	0.001	0.0	0.0	0.0
116	10.035	3.363	7.490	84.5	58.3	92.7
117	0.164	0.418	0.000	1.4	7.2	0.0
Total	11.88	5.77	8.08	100	100	100

which has the highest feeding rate of methanol, as expected. The amino acids were most effectively synthesized in this condition, only Cys was supplied through catabolism reactions in Period III (Table I). The amino acid of central importance, Glu, again had the highest synthesis flux (1.20 mmol/g DW/h in Period II) compared to the other amino acids. The nucleotide synthesis pathway fluxes (R92–110) were the highest of all conditions in Period II of MS-0.04 condition. Moreover, the synthesis fluxes for one-carbon units (R111–115), carbohydrates (R127), and lipids (R128–138) were the highest of all conditions in Periods II and III of MS-0.04 condition, with an average of 1.5-fold higher fluxes, due to the higher specific growth rate. Thus, the cells fed with higher inlet rates of methanol had higher synthesis fluxes for byproducts in later periods of the bioprocess.

In Periods I and III, as compared to other conditions, the highest ATP synthesis flux was achieved, where most ATP was supplied by oxidative phosphorylation (Table II). Moreover, the highest rHuEPO synthesis flux (R140 = 0.0103 μmol/g DW/h) and the highest maintenance energy requirement (R141 = 16.40 mmol/g DW/h) were attained in Period I, compared to other conditions. On the other hand, in Period II, substrate-level phosphorylation had a higher impact, and ATP was not wasted for maintenance energy requirements.

Metabolic Flux Distribution at Principal Nodes

Comparison of the normalized metabolic flux distributions at the pyruvate node (in Period III), and at glyceraldehyde-3-phosphate node (in Period II), with different feeding conditions are given in Figure 4. The principal nodes were selected as those metabolic branch points, where significant changes in flux partitioning would highly effect product yield, and Pyr is a generally accepted candidate (Stephanopoulos and Vallino, 1991), whereas G3P node was selected for its importance in methanol metabolism, which directly affects r-protein yield. The normalization was

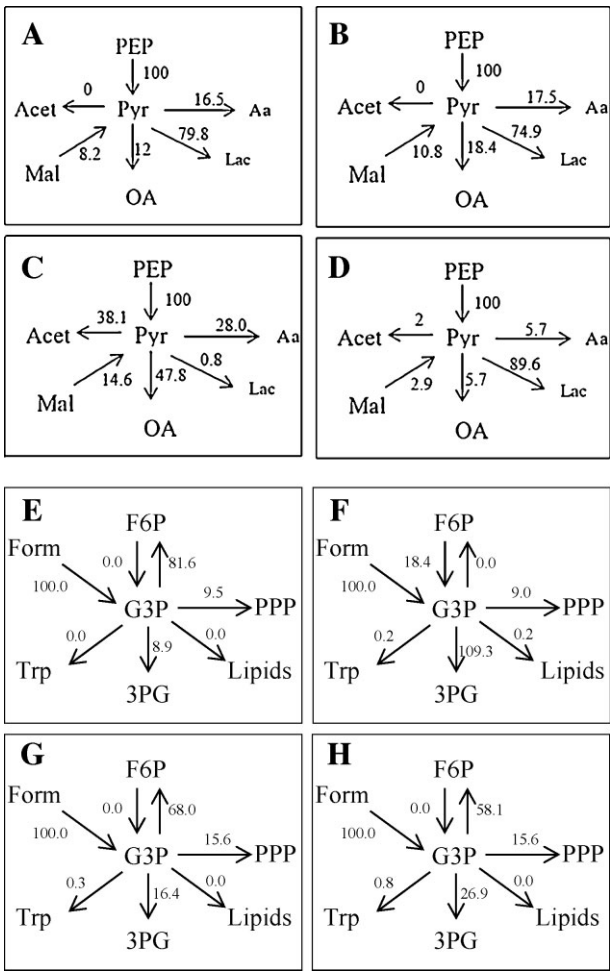

Figure 4. Normalized metabolic flux distributions at Pyr (at $t = 15$ h) and G3P (at $t = 9$ h) nodes for the bioprocesses with different with feeding conditions. **A** and **E**: M-0.03 condition; **B** and **F**: MS-0.03 condition; **C** and **G**: MS-0.04 condition; **D** and **H**: MS-0.02 condition.

performed by assigning 100% to the flux for the reactions R14 and R4 respectively, and calculating the other fluxes accordingly. Thus, all incoming fluxes to a node equals all outgoing fluxes from a node, as seen in Figure 4.

The incoming flux to the pyruvate node was replenished by the anaplerotic pathway from malate, with the highest rate being in the MS-0.04 condition during Period III (Fig. 4C). In the same condition, more of the pyruvate was used in the TCA cycle and the formation of certain amino acids (Ala, Val, Ile, and Trp) and, considering all the branches of the metabolism, least was spent on byproduct formation. Moreover, the byproduct distribution was different than in the other three conditions. Thus, considering only the Pyr node in Period III, MS-0.04 condition seems to be the most favorable, in terms of desirable distribution of fluxes towards r-protein production.

Although lactate is a byproduct for r-protein production and diminishes in sorbitol supplemented medium (Fig. 4C), the overexpression of lactate (Çelik et al., 2009) could be industrially important. If investigated in more detail, this could lead to circumventing the currently observed problems in microbial production of lactate (Kern et al., 2007), which is gaining importance as the raw material of biodegradable and renewable plastics; rendering the *P. pastoris* expression system as a possible alternative for the industrially valuable lactate production.

Formaldehyde entering the metabolism from glyceraldehyde-3-phosphate node was supported by the other carbon source, sorbitol; hence in Period II, the highest flux from the G3P node towards the glycolysis cycle and the lowest flux towards the PPP compared to the other conditions was obtained for MS-0.03 condition (Fig. 4F). Thus, considering only the G3P node in Period II, MS-0.03 condition seems to be the most favorable, to obtain desirable distribution of fluxes towards r-protein production.

Both Pyr and G3P nodes were flexible (Fig. 4), and could adapt to changes in methanol feeding rate.

Conclusion

As product and by-product formation in the bioprocess for the rHuEPO production are dependent on the carbon source, the effects of different feeding conditions on the intracellular reaction rate distributions in r-protein production by *P. pastoris* were investigated by MFA, based on a detailed description of the stoichiometry of all relevant bioreactions involved. The stoichiometric model constructed for this purpose consisted of $m = 102$ metabolites and $n = 141$ reactions.

Considering the methanol utilization pathway, after methanol was converted to formaldehyde (R1), almost all of the formaldehyde (>99%) entered the assimilatory pathway (via R4). Only in the MS-0.02 condition was it converted to other metabolites, rather than being discarded by the dissimilatory pathway (R2–R3), in all the periods of the process (Fig. 3). This shows that the methanol feed did not exceed the cell requirements in this condition. Moreover, the distribution of fluxes between the assimilatory and the dissimilatory pathways were similar for M-0.03 and MS-0.02 conditions. However, there was a shift in the metabolism for the MS-0.03 and MS-0.04 conditions, as seen in Figure 3, pointing to the fact that the methanol feed was in excess of the metabolic requirements for these two conditions.

The glycolysis, gluconeogenesis, and PPP pathways worked uninterruptedly in all the periods, only for MS-0.02 condition. Moreover, in the MS-0.02 condition, the nucleotide, carbohydrate, and lipid synthesis pathway fluxes in Period I were the highest of all conditions. On the other hand, the highest rHuEPO synthesis flux in Period II was obtained for MS-0.02 condition ($R140 = 0.0068$ μmol/g DW/h), which was twice the flux for M-0.03 condition. Thus, the MS-0.02 condition, where methanol was fed at a predetermined rate such that $\mu_0 = 0.02\ h^{-1}$ and sorbitol was

added batch-wise at a concentration $C_{S0} = 50$ g/L, proves to be a remarkably advantageous condition for r-protein production with *P. pastoris*; since methanol and oxygen requirements are lowered, and the stress on the cell due to methanol toxicity has been removed.

On the other hand, comparing M-0.03 and MS-0.03 conditions to see the sole effect of sorbitol addition, where both conditions had the same methanol feed rates, addition of sorbitol increased the rHuEPO synthesis flux as high as 4.4-fold (in Period I). Notably, the methanol feed rate did not significantly affect the sorbitol flux (R5).

In none of the feeding conditions, was the TCA cycle complete for all process periods, probably due to oxygen supply not meeting the oxygen demand—a common problem for *P. pastoris* fermentations. Moreover, PPP and TCA cycles worked with highest disturbances at MS-0.04 condition, which shows the stress of increased feeding rates of methanol on cell metabolism. The amino acid of central importance, Glu, generally had the highest synthesis flux, and Cys had the lowest. Tyrosine was not synthesized throughout the bioprocess in MS-0.02 condition, but was supplied through catabolism reaction R84. Thus, adding tyrosine to the medium in MS-0.02 condition could be helpful in improving the protein synthesis pathway, and eliminating the metabolic bottleneck.

An analysis of the normalized fluxes at principal nodes of the metabolism was also performed. Considering only the Pyr node in Period III, the MS-0.04 condition seemed to be the most favorable; and considering only the G3P node in Period II, MS-0.03 condition was the most favorable condition, in terms of desirable distribution of fluxes towards r-protein production. Nevertheless, the overall scenario is more important for therapeutic protein production, where priority is given to the conditions increasing the production rates of the recombinant protein. In this context, optimization according to principal node analysis does not prove to be very consistent or helpful.

Briefly, this study points, for the first time, to the metabolic basis of the support provided by the co-substrate (sorbitol) proposed for *P. pastoris* Mut^+ strains. It has used intracellular reaction rates to explain the decrease in oxygen and methanol requirements of the cell for simultaneous growth and r-protein production. Although the optimum process conditions would change according to the desired scale, quality and type of the product, the in-depth insight provided will certainly be helpful in the production of other r-proteins by *P. pastoris*, which has become a popular microbial production system in the last decade.

This work was supported by the Scientific and Technological Research Council of Turkey (TÜBİTAK) through the project 107M285 and METU Research Fund, and by a Grant to SGO under the BRIC initiative of the UK Biotechnology & Biological Sciences Research Council. E.Ç. was awarded scholarships by Scientific and Technical Research Council of Turkey (TÜBİTAK-BİDEB). Professor Tunçer H. Özdamar (Ankara Univ), Professor İsmail Tosun (METU), and Dr Juan Castrillo are warmly acknowledged for their contributions.

Appendix: Metabolic Reactions for *P. pastoris*

Methanol Metabolism

1. $MeOH \rightarrow Form$
2. $Form \rightarrow For + NADH$
3. $For \rightarrow NADH + CO_2$
4. $Xyl5P + Form + ATP \rightarrow ADP + 2G3P$

Sorbitol Metabolism

5. $Sorb + ATP \rightarrow ADP + F6P + NADH$

Glycolysis and Gluconeogenesis Pathway

6. $F6P \rightarrow G6P$
7. $G6P \rightarrow F6P$
8. $F6P + ATP \rightarrow 2G3P + ADP$
9. $2G3P \rightarrow F6P + Pi$
10. $G3P + ADP + Pi \rightarrow 3PG + ATP + NADH$
11. $3PG + ATP + NADH \rightarrow G3P + ADP + Pi$
12. $3PG \rightarrow PEP$
13. $PEP \rightarrow 3PG$
14. $PEP + ADP \rightarrow Pyr + ATP$
15. $Pyr \rightarrow AcCoAm + CO_2 + NADHm$

Pentose Phosphate Pathway

16. $G6P \rightarrow R5P + 2NADPH + CO_2$
17. $R5P \rightarrow Xyl5P$
18. $Xyl5P \rightarrow R5P$
19. $R5P \rightarrow Rib5P$
20. $Rib5P \rightarrow R5P$
21. $Xyl5P + Rib5P \rightarrow S7P + G3P$
22. $S7P + G3P \rightarrow Xyl5P + Rib5P$
23. $Xyl5P + E4P \rightarrow F6P + G3P$
24. $F6P + G3P \rightarrow Xyl5P + E4P$
25. $G3P + S7P \rightarrow F6P + E4P$
26. $F6P + E4P \rightarrow G3P + S7P$

Branches From Glycolysis Pathway

27. $Pyr \rightarrow Acet + CO_2$
28. $Acet \rightarrow Ac + NADPH$
29. $Acet + NADH \rightarrow EtOH$
30. $Ac + 2ATP \rightarrow AcCoA + 2ADP + 2Pi$
31. $AcCoA \rightarrow AcCoAm$
32. $Pyr + NADH \rightarrow Lac$
33. $Lac \rightarrow NADH + Pyr$

Anaplerotic Reactions

34. $Mal \rightarrow Pyr + CO_2 + NADPHm$
35. $Pyr + CO_2 + ATP \rightarrow OA + ADP$
36. $OA + ATP \rightarrow PEP + ADP + CO_2$

TCA Cycle

37. $AcCoAm + OA \rightarrow Cit$
38. $Cit \rightarrow ICit$
39. $ICit \rightarrow \alpha KG + CO_2 + NADHm$
40. $\alpha KG \rightarrow SucCoA + CO_2 + NADHm$
41. $SucCoA + Pi + ADP \rightarrow Suc + ATP$
42. $Suc + ATP \rightarrow SucCoA + ADP + Pi$
43. $Suc \rightarrow Fum + FADH_2$
44. $Fum \rightarrow Mal$
45. $Mal \rightarrow Fum$
46. $Mal \rightarrow OA + NADHm$
47. $NADH_m + OA \rightarrow Mal$

Biosynthesis of Serine Family Amino Acids

48. $3PG + Glu \rightarrow Ser + \alpha KG + NADH + Pi$
49. $Ser + THF \rightarrow Gly + MetTHF$
50. $Ser + AcCoA + H_2S \rightarrow Cys$

Biosynthesis of Alanine Family Amino Acids

51. $Pyr + Glu \rightarrow Ala + \alpha KG$
52. $2Pyr + NADPHm \rightarrow Kval + CO_2$
53. $Kval + Glu \rightarrow Val + \alpha KG$
54. $Kval + AcCoAm + Glu \rightarrow Leu + \alpha KG + NADH + CO_2$

Biosynthesis of Histidine

55. $R5P + ATP \rightarrow PRPP + AMP$
56. $PRPP + ATP + Gln \rightarrow His + PRAIC + \alpha KG + 2PPi$ -
    $aKG + 2PPi + 2NADH + Pi$

Biosynthesis of Aspartic Family Amino Acids

57. $OA + Glu \rightarrow Asp + \alpha KG$
58. $Asp + Gln + ATP \rightarrow Asn + Glu + AMP + PPi$
59. $Asp + ATP + 2NADPH \rightarrow Hser + ADP + Pi$
60. $HSer + ATP \rightarrow Thr + ADP + Pi$
61. $Thr + NADPHm +$ -
    $+ Glu + Pyr \rightarrow Ile + \alpha KG + NH_4 + CO_2$
62. $AcCoA + HSer + H_2S + MTHF \rightarrow Met + THF$

Biosynthesis of Aromatic Family Amino Acids

63. $2PEP + E4P + ATP + NADPH \rightarrow Chor + ADP + 4Pi$
64. $Chor + Glu \rightarrow Phe + \alpha KG + CO_2$
65. $Chor + Glu \rightarrow Tyr + \alpha KG + NADH + CO_2$
66. $Chor + Gln + PRPP + Ser \rightarrow Trp + Glu + Pyr + G3P$ -
    $+ Glu + Pyr + G3P + CO_2 + PPi$

Biosynthesis of Glutamic Family Amino Acids

67. $\alpha KG + NH_4 + NADPH \rightarrow Glu$
68. $Glu + ATP + NH_4 \rightarrow Gln + ADP + Pi$
69. $Glu + ATP + 2NADPH \rightarrow Pro + ADP + Pi$
70. $Gln + CO_2 + 2ATP \rightarrow CaP + Glu + 2ADP + Pi$
71. $2Glu + AcCoAm + 4ATP + NADPHm + CaP + Asp$ -
    $CaP+Asp\backslash rightarrow Arg+\alpha K\Gamma+4ADP+Fum+$-
    $\rightarrow Arg + \alpha KG + 4ADP + Fum + 5Pi$
72. $2Glu + AcCoA + 3ATP + 2NADPH \rightarrow Lys + \alpha KG +$ -
    $\alpha KG + CO_2 + 2NADH$

Catabolism of Amino Acids

73. $Ala + \alpha KG \rightarrow Pyr + Glu$
74. $Arg + \alpha KG + NADPH \rightarrow Glu + 2NH_4 + CO_2$
75. $Asn \rightarrow Asp + NH_4$
76. $Asp + \alpha KG + NADH \rightarrow Glu + Mal$
77. $Cys \rightarrow Pyr + NH_4 + H_2S$
78. $Gln \rightarrow Glu + NH_4$
79. $Glu \rightarrow NH_4 + NADH + \alpha KG$
80. $Gly + MetTHF \rightarrow Ser + THF$
81. $His + THF \rightarrow Glu + F10THF + NH_4$
82. $Ile + \alpha KG \rightarrow Glu + FADH_2 + 2NADH + CO_2 + AcCo$-
    $2NADH + CO_2 + AcCoA + SucCoA$
83. $Leu + \alpha KG + ATP \rightarrow Glu + FADH_2 + NADH + 2AcC$-
    $FADH_2 + NADH + 2AcCoA + ADP + Pi$
84. $Phe + NADH \rightarrow Tyr$
85. $Pro \rightarrow Glu + NADH + FADH_2$
86. $Ser \rightarrow Pyr + NH_4$
87. $Thr \rightarrow Gly + NADH + AcCoA$
88. $Trp + NADPH \rightarrow 2AcCoA + Ala + CO_2 + NH_4 + For$ -
    $+ NH_4 + For + 2NADH + FADH_2$
89. $Tyr + \alpha KG \rightarrow Glu + Fum + 2AcCoA + CO_2$
90. $Val + \alpha KG + ATP \rightarrow Glu + FADH_2 + 3NADH + CO_2$ -
    $+ 3NADH + CO_2 + SucCoA$
91. $Lys + AcCoA + 2\alpha KG \rightarrow 2Glu + NADH + CO_2$

Biosynthesis of Nucleotides

92. $PRPP + 2Gln + Asp + CO_2 + Gly + 4ATP + F10TH$-
    $Gly + 4ATP + F10THF \rightarrow 2Glu + PPi + 4ADP + 4Pi$ -
    $PPi + 4ADP + 4Pi + THF + PRAIC + Fum$
93. $PRAIC + F10THF \rightarrow IMP + THF$
94. $IMP + Gln + ATP \rightarrow NADH + GMP + Glu + AMP$ -
    $GMP + Glu + AMP + PPi$
95. $GMP + ATP \rightarrow GDP + ADP$
96. $ATP + GDP \rightarrow ADP + GTP$
97. $GTP + ADP \rightarrow ATP + GDP$
98. $NADPH + ATP \rightarrow dATP$
99. $NADPH + GDP + ATP \rightarrow dGTP + ADP$
100. $IMP + GTP + Asp \rightarrow GDP + Pi + Fum + AMP$
101. $AMP + ATP \rightarrow 2ADP$
102. $PRPP + Asp + CaP \rightarrow UMP + NADH + PPi + Pi +$ -
     $NADH + PPi + Pi + CO_2$

103. UMP + ATP → UDP + ADP
104. UDP + ATP → ADP + UTP
105. UTP + NH_4 + ATP → CTP + ADP + Pi
106. CTP + ADP → CDP + ATP
107. CDP + ATP → CTP + ADP
108. CDP + ADP → CMP + ATP
109. ATP + NADPH + CDP → dCTP + ADP
110. UDP + MetTHF + 3ATP + NADPH → dTTP + DH-
→ dTTP + DHF + 3ADP + Ppi + Pi

Biosynthesis and Interconversion of One-Carbon Units

111. DHF + NADPH → THF
112. Gly + THF → MetTHF + NH_4 + NADH + CO_2
113. MetTHF + NADH → MTHF
114. MetTHF → MeTHF + NADPH
115. MeTHF → F10THF

Oxidative Phosphorylation (*P/O* = 2)

116. NADHm + 2ADP + 2Pi → 2ATP
117. $FADH_2$ + ADP + Pi → ATP

Transport Reactions

118. CO_2 → exp
119. imp → CO_2
120. imp → NH_4
121. NH_4 → exp
122. 2ATP + 4NADPH → AMP + ADP + H_2S + PPi + Pi
123. PPi → 2Pi
124. imp → Pi
125. Pi → exp
126. NADH → NADHm

Biosynthesis of Carbohydrate

127. ATP + G6P → ADP + 6CARBH + 2Pi

Biosynthesis of Lipids

128. ACCoA + ATP + CO_2 → ADP + MaCoA + Pi
129. ACCoA + 7MaCoA + 14NADPH → 7CO_2 + PLM
130. NADPH + PLM + ATP → PLLM
131. ACCoA + 8MaCoA + 16NADPH → 8CO_2 + STE
132. NADPH + STE + ATP → OLE
133. 1.7OLE + 4.4PLLM + 1.4PLM + STE → 8.5FA
134. 2FA + G3P → PA
135. CTP + PA + Ser → 2Pi + CMP + PS
136. PS → CO_2 + PE
137. PE + 3ATP + 3Met → PC + 3AcCoA + 3H_2S + 3HSe-
3AcCoA + 3H_2S + 3HSer + 9Pi
138. PA + CTP + G6P → CMP + PINS

Biomass Synthesis

139. 0.459Ala + 0.161Arg + 0.102Asn + 0.297Asp + 0.007-
+ 0.297Asp + 0.007Cys + 0.105Gln + 0.302Glu -
+ 0.302Glu + 0.290-
0.290Gly + 0.066His + 0.193Ile + 0.296Leu + 0.286L-
+ 0.296Leu + 0.286Lys + 0.051Met + 0.134Phe -
+ 0.134Phe + 0.165-
0.165Pro + 0.185Ser + 0.191Thr + 0.028Trp + 0.102-
+ 0.028Trp + 0.102Tyr + 0.265Val + 0.051AMP -
+ 0.051AMP + 0.051GMP + 0.067UMP + 0.05CMP -
+ 0.05CMP + 0.0024dATP + 0.0016dGTP + 0.0016d-
0.0016dGTP + 0.0016dTTP + 0.0024dCTP + 0.0101-
0.0024dCTP + 0.0101OLE + 0.0081PLM
+0.0263PLLM + 0.0061STE + 0.0006PA + 0.005PIN-
0.0006PA + 0.005PINS + 0.002PS + 0.005PE + 0.006-
+ 0.005PE + 0.006PC + 2.5CARBH + 23.917ATP → -
23.917ATP → Biomass + 23.917ADP + 23.946Pi

Erythropoietin Synthesis

140. 34Ala + 15Arg + 11Asn + 10Asp + 4Cys + 8Gln + 24-
4Cys + 8Gln + 24Glu + 14-
24Glu + 14-
14Gly + 8His + 12Ile + 30Leu + 9Lys + 2Met + 11P-
9Lys + 2Met + 11Phe + 12Pro + 18Ser + 19Thr + 3-
18Ser + 19Thr + 3Trp + 5Tyr + 17Val + 1064ATP -
17Val + 1064ATP → EPO + 1064ADP + 1064Pi

Maintenance Energy

141. ATP → ADP + Pi

References

Antoniewicz MR, Kraynie DF, Laffend LA, Gonzalez-Lergier J, Kelleher JK, Stephanopoulos G. 2007. Metabolic flux analysis in a nonstationary system: Fed-batch fermentation of a high yielding strain of *E. coli* producing 1,3-propanediol. Metab Eng 9:277–292.

Bonora A, Mares D. 1982. A simple colorimetric method for detecting cell viability in cultures of eukaryotic microorganisms. Curr Microbiol 7:217–222.

Bradford MM. 1976. A rapid and sensitive for the quantitation of microgram quantities of protein utilizing the principle of protein dye binding. Anal Biochem 72:248–254.

Brierley RA, Bussineau C, Kosson R, Melton A, Siegel RS. 1990. Fermentation development of recombinant *Pichia pastoris* expressing the heterologous gene: Bovine lysozyme. Ann NY Acad Sci 589:350–362.

Çalık P, Özdamar TH. 1999. Mass flux balance-based model and metabolic pathway analysis for serine alkaline protease synthesis by *Bacillus licheniformis*. Enzyme Microb Tech 24:621–635.

Çalık P, Özdamar TH. 2002a. Bioreaction network flux analysis for industrial microorganisms: A review. Rev Chem Eng 18:553–596.

Çalık P, Özdamar TH. 2002b. Metabolic flux analysis for human therapeutic protein productions and hypothesis for new therapeutical strategies in medicine. Biochem Eng J 11:49–68.

Çalık P, Çalık G, Özdamar TH. 1998. Oxygen transfer effects in serine alkaline protease fermentation by *Bacillus licheniformis*: Use of citric acid as the carbon source. Enzyme Microb Tech 23:451–461.

Çalık P, Çalık G, Takaç S, Özdamar TH. 1999. Metabolic flux analysis for serine alkaline protease fermentation by *Bacillus licheniformis* in a defined medium: Effects of the oxygen transfer rate. Biotechnol Bioeng 64:151–167.

Çelik E, Çalık P, Halloran SM, Oliver SG. 2007. Production of recombinant human erythropoietin from *Pichia pastoris* and its structural analysis. J Appl Microbiol 103:2084–2094.

Çelik E, Özbay N, Oktar N, Çalık P. 2008. Use of biodiesel by-product crude glycerol as the carbon source for fermentation processes by recombinant *Pichia pastoris*. Ind Eng Chem Res 47:2985–2990.

Çelik E, Çalık P, Oliver SG. 2009. Fed-batch methanol feeding strategy for recombinant protein production by *Pichia pastoris* in the presence of co-substrate sorbitol. Yeast 26:473–484.

Cereghino JL, Cregg JM. 2000. Heterologous protein expression in the methylotrophic yeast *Pichia pastoris*. FEMS Microb Rev 24:45–66.

Chen W, Hughes DE, Bailey JE. 1994. Intracellular expression of Vitreoscilla hemoglobin alters the aerobic metabolism of Saccharomyces cerevisiae. Biotechnol Prog 10:308–313.

De Schutter K, Lin YC, Tiels P, Van Hecke A, Glinka S, Weber-Lehmann J, Rouzé P, Van de Peer Y, Callewaert N. 2009. Genome sequence of the recombinant protein production host *Pichia pastoris*. Nat Biotechnol 27:561–566.

Fiaux J, Çakar ZP, Sonderegger M, Wuthrich K, Szyperski T, Sauer U. 2003. Metabolic-flux profiling of the yeasts *Saccharomyces cerevisiae* and *Pichia stipitis*. Eukaryot Cell 2:170–180.

Förster J, Gombert AK, Nielsen J. 2002. A functional genomics approach using metabolomics and in silico pathway analysis. Biotechnol Bioeng 79:703–712.

Förster J, Famili I, Fu P, Palson BO, Nielsen J. 2003. Genome-scale reconstruction of the *Saccharomyces cerevisiae* metabolic network. Genome Res 13:244–253.

Gonzalez R, Andrews BA, Molitor J, Asenjo JA. 2003. Metabolic analysis of the synthesis of high levels of intracellular human SOD in *Saccharomyces cerevisiae* rhSOD 2060 411 SGA122. Biotechnol Bioeng 82:152–169.

Hellwig S, Emde F, Raven NPG, Henke M, Van der Logt P, Fischer R. 2001. Analysis of single chain antibody production in *Pichia pastoris* using on-line methanol control in fed-batch and mixed-feed fermentation. Biotechnol Bioeng 74:344–352.

İleri N, Çalık P. 2006. Effects of pH strategy on endo- and exo-metabolome profiles and sodium potassium hydrogen ports of beta-lactamase producing *Bacillus licheniformis*. Biotechnol Prog 22:411–419.

Inan M, Meagher MM. 2001. Non-repressing carbon sources for alcohol oxidase (AOX1) promoter of *Pichia pastoris*. J Biosci Bioeng 92:585–589.

Jorgensen H, Nielsen J, Villadsen J, Mollgaard H. 1995. Metabolic flux distributions in Penicillium chrysogenum during fed-batch cultivations. Biotechnol Bioeng 46:117–131.

Jungo C, Schenk J, Pasquier M, Marison IW, von Stockar U. 2007. A quantitative analysis of the benefits of mixed feeds of sorbitol and methanol for the production of recombinant avidin with *Pichia pastoris*. J Biotechnol 131:57–66.

Kern A, Tilley E, Hunter IS, Legisa M, Glieder A. 2007. Engineering primary metabolic pathways of industrial micro-organisms. J Biotechnol 129:6–29.

Kresnowati MTAP, van Winden WA, van Gulik WM, Heijnen JJ. 2008. Dynamic in vivo metabolome response of *Saccharomyces cerevisiae* to a stepwise perturbation of the ATP requirement for Benzoate Export. Biotechnol Bioeng 99:421–441.

Maaheimo H, Fiaux J, Cakar ZP, Bailey JE, Sauer U, Szyperski T. 2001. Central carbon metabolism of *Saccharomyces cerevisiae* explored by biosynthetic fractional ^{13}C labeling of common amino acids. Eur J Biochem 268:2464–2479.

Mathews CK, van Holde KE. 1996. Biochemistry, 2nd edn, USA: Benjamin-Cummings Pub Co.

Nielsen J, Villadsen J, Liden G. 2003. Bioreaction engineering principles. New York: Kluwer Academic Pub.

Nöh K, Grönke K, Luo B, Takors R, Oldiges M, Wiechert W. 2007. Metabolic flux analysis at ultra short time scale: Isotopically non-stationary 13C labeling experiments. J Biotechnol 129:249–267.

Ramon R, Ferrer P, Valero F. 2007. Sorbitol co-feeding reduces metabolic burden caused by theoverexpression of a *Rhizopus oryzae* lipase in *Pichia pastoris*. J Biotechnol 130:39–46.

Sola A, Maaheimo H, Ylonen K, Ferrer P, Szyperski T. 2004. Amino acid biosynthesis and metabolic flux profiling of *Pichia pastoris*. Eur J Biochem 271:2462–2470.

Sola A, Jouhten P, Maaheimo H, Sanchez-Ferrando F, Szyperski T, Ferrer P. 2007. Metabolic flux profiling of *Pichia pastoris* grown on glycerol/methanol mixtures in chemostat cultures at low and high dilution rates. Microbiology 153:281–290.

Sreekrishna K, Brankamp RG, Kroop KE, Blankenship DT, Tsay JT, Smith PL, Wierschke JD, Subramaniam A, Birkenberger LA. 1997. Strategies for optimal synthesis and secretion of heterologous proteins in the methylotrophic yeast *Pichia pastoris*. Gene 190:55–62.

Stephanopoulos G, Vallino JJ. 1991. Network rigidity and metabolic engineering in metabolite overproduction. Science 252:1675–1681.

Toivari MH, Aristidou A, Ruohonen L, Penttilä M. 2001. Conversion of xylose to ethanol by recombinant Saccharomyces cerevisiae: Importance of xylulokinase (XKS1) and oxygen availability. Metab Eng 3:236–249.

Tsai PS, Hatzimanikatis V, Bailey JE. 1996. Effect of Vitreoscilla hemoglobin dosage on microaerobic Escherichia coli carbon and energy metabolism. Biotechnol Bioeng 49:139–150.

Van De Walle M, Shiloach J. 1998. Proposed mechanism of acetate accumulation in two recombinant *Escherichia coli* strains during high density fermentation. Biotechnol Bioeng 57:71–78.

Van Wegen RJ, Lee S-Y, Middelberg APJ. 2001. Metabolic and kinetic analysis of poly(3-Hydroxybutyrate) production by recombinant *Escherichia coli*. Biotechnol Bioeng 74:70–80.

Xie J, Zhou Q, Du P, Gan R, Ye Q. 2005. Use of different carbon sources in cultivation of recombinant *Pichia pastoris* for angiostatin production. Enzyme Microb Tech 36:210–216.